Environmental Science & Technology Letters

Letter

Cite This: Environ. Sci. Technol. Lett. 2018, 5, 436−441

pubs.acs.org/journal/estlcu

Effect of Model Spatial Resolution on Estimates of Fine Particulate Matter Exposure and Exposure Disparities in the United States

David A. Paolella,[†] Christopher W. Tessum,*[,†] Peter J. Adams,[‡] Joshua S. Apte,[§] Sarah Chambliss,[§] Jason Hill,[∥] Nicholas Z. Muller,[⊥] and Julian D. Marshall[†]

[†]Department of Civil and Environmental Engineering, University of Washington, Seattle, Washington 98195, United States

[‡]Department of Civil and Environmental Engineering, Carnegie Mellon University, Pittsburgh, Pennsylvania 15213, United States

[§]Department of Civil, Architectural and Environmental Engineering, The University of Texas at Austin, Austin, Texas 78712, United States

[∥]Department of Bioproducts and Biosystems Engineering, University of Minnesota, St. Paul, Minnesota 55108, United States

[⊥]Department of Engineering and Public Policy, Tepper School of Business, Carnegie Mellon University, Pittsburgh, Pennsylvania 15213, United States

Supporting Information

ABSTRACT: To the extent that pollution and population are spatially correlated, air quality modeling with coarse-resolution horizontal grids may systematically underpredict exposures and disparities in exposure among demographic groups (i.e., environmental injustice). We use InMAP, a reduced-complexity air pollution model, to quantify how estimates of year-2014 fine particulate matter ($PM_{2.5}$) exposure in the United States vary with model spatial resolution, for a variable-resolution grid. We test five grids, with population-weighted average grid cell edge lengths ranging from 5.9 to 69 km. We find that model-estimated $PM_{2.5}$ exposure, and exposure disparities among racial-ethnic groups, are lower with coarse grids than with fine grids: switching from our coarsest- to finest-resolution grid increases the calculated population-weighted average exposure by 27% (from 6.6 to 8.3 $\mu g\ m^{-3}$) and causes the estimated difference in average exposure between minorities and whites to increase substantially (from 0.4 to 1.6 $\mu g\ m^{-3}$). Across all grid resolutions, exposure disparities by race-ethnicity can be detected in every income category. Exposure disparities by income alone remain small relative to disparities by race-ethnicity, irrespective of resolution. These results demonstrate the importance of fine model spatial resolution for identifying and quantifying exposure disparity.

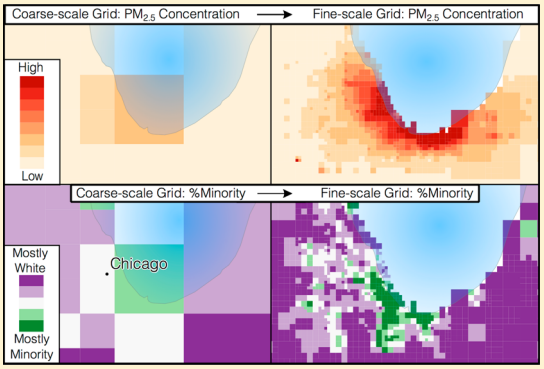

INTRODUCTION

Ambient air pollution accounts for an estimated 4 million premature deaths per year worldwide, with fine particulate matter ($PM_{2.5}$) being the main contributor.[1] Despite progress in reducing air pollution, $PM_{2.5}$ remains a substantial health concern in the United States, causing nearly 100000 premature deaths in 2016.[2] No "safe" level of $PM_{2.5}$ has been found.[3−7] Di et al.[8] reported significant adverse health effects from exposure to $PM_{2.5}$ at concentrations below the current national standard (12 $\mu g\ m^{-3}$) and found a larger dose−response relationship for self-identified racial minorities and people with low income.

Racial-ethnic and socioeconomic disparities in exposure to air pollution, often termed environmental injustice, are well-documented.[9−19] A 1994 Executive Order directed each U.S. federal agency to incorporate environmental justice into its mission by addressing "disproportionately high and adverse human health or environmental effects of its programs, policies, and activities on minority populations and low-income populations".[20] Consequently, there is a need for assessments of potential emissions scenarios to estimate not only population-wide impacts of changes in air quality but also the distributional equity of impacts among population subgroups.

Relating potential changes in emissions to $PM_{2.5}$ health impacts generally requires the use of mechanistic air pollution models. Such models typically divide a spatial domain into discrete grid cells to simulate air pollution emission, transport, transformation, and removal. For a given spatial domain, computational expense is inversely related to the volume of each grid cell. Available computational resources generally limit the spatial resolution of a simulation. Because models usually assume that the atmosphere is homogeneous within each grid cell, emissions occurring at any point within a cell are

Received: May 29, 2018
Revised: June 18, 2018
Accepted: June 19, 2018
Published: June 19, 2018

DOI: 10.1021/acs.estlett.8b00279
Environ. Sci. Technol. Lett. 2018, 5, 436−441

assumed to mix instantaneously throughout the whole volume. Therefore, to the extent that population and $PM_{2.5}$ are spatially correlated, air quality modeling with a coarse-resolution grid could cause modeled pollution to be artificially (and incorrectly) diluted away from nearby populations, resulting in a tendency to underestimate $PM_{2.5}$ exposures and exposure disparities.

Previous studies (see Table S1) have investigated the effects of horizontal grid resolution on the ability of a model to match $PM_{2.5}$ monitor measurements. The applicability of those studies to human exposure or exposure disparities depends on whether monitor locations are a good surrogate for population. Other studies have measured the sensitivity of modeled population-wide health impacts of $PM_{2.5}$ to grid resolution (see Table S1), with some providing evidence that coarse spatial resolution causes underestimates of $PM_{2.5}$ concentrations and corresponding impacts on mortality, especially in cities where concentration and population gradients are steep.[21−23] As a notable exception, Thompson et al.[24] found that grid resolution did not affect estimates of health impacts due to total $PM_{2.5}$ in nine regions in the eastern United States; however, they noted that estimated impacts of primary $PM_{2.5}$, accounting for a small fraction of total impacts relative to secondary $PM_{2.5}$ in their scenario, did increase with finer resolution. Secondary $PM_{2.5}$, which (formed from emissions of gases) typically has spatial gradients smaller than those of primary $PM_{2.5}$, is less likely to be sensitive to spatial resolution.[25] None of the prior studies combined the fine spatial resolution necessary to model neighborhood-scale variation with full coverage of the contiguous United States.

In addition, to the best of our knowledge, no previous study has investigated how modeled environmental injustice in $PM_{2.5}$ exposure varies by grid cell size. Saari et al.,[26] however, investigated this question for ozone; they assessed the impact of varying model resolution on estimated ozone-related mortality by household income category and found only a minor effect in one study region.

As part of the CACES (Center for Air, Climate, and Energy Solutions) EPA-ACE Center, this paper aims to fill these gaps in the literature, as noted above, by quantifying the effect of model spatial resolution on estimates of $PM_{2.5}$ exposure and exposure disparities by race-ethnicity and income across the entire contiguous United States. The results demonstrate the potential effect of model spatial resolution on the estimated environmental justice impacts of future emissions scenarios.

MATERIALS AND METHODS

We employ InMAP (Intervention Model for Air Pollution), a reduced-complexity national-scale air quality model with flexible grid resolution that allows computational resources to be dedicated to areas that have highly spatially variable pollutant concentrations and population densities.[27] InMAP estimates annual-average concentrations of fine particulate matter based on emissions of volatile organic compounds (VOCs), nitrogen oxides (NO_x), ammonia (NH_3), sulfur dioxide (SO_2), and primary $PM_{2.5}$. Emissions inputs to InMAP include year-2014 anthropogenic sources from the 2014 National Emissions Inventory (NEI),[28] supplemented with year-2005 NEI biogenic and fire sources that were unavailable in the current inventory.

NEI emissions data consist of point and area sources. For each grid tested, point sources are allocated to the grid cells with which they intersect, allowing the spatial resolution of emissions to match the InMAP grid resolution. Though area source emissions are provided as county totals, the NEI provides spatial surrogates that can be used to apportion the county emissions to grid cells, following the approach used by SMOKE.[29] Spatial surrogate factors vary by emissions source and are based on spatial data (e.g., population, land cover, or road networks) at resolutions finer than those of the county data, such as Census Tracts, Block Groups, or linear data, with a spatial resolution that is typically <1 km^2 in urban areas. We used these spatial surrogates and the InMAP Air Emissions Processor[30] to allocate county-based emissions to grid cells.

Population data are from the U.S. Census Bureau 2012−2016 American Community Survey (ACS) at the Census Block Group level of spatial aggregation.[31] We focus on the four largest race-ethnicity groups determined by self-identification in the Census: Asian, black, Latino, and white. We aggregate these four population subgroups such that they are mutually exclusive. "Latino" includes people of all races who identify as having Hispanic or Latino origin; the other three groups (Asian, black, and white) refer only to non-Latino/non-Hispanic persons. See Table S2 for the population distribution by race-ethnicity.

The 2012−2016 ACS provides income statistics by Census Tract, with 16 household income categories (lowest, less than $10000; highest, $200000 or more). We use the proportion of households in each income category to estimate population counts (see Table S3 for the population distribution by income) at the finest available level of race-ethnicity information: white and minority (i.e., the combination of Asian, black, Latino, and all other groups not identifying as white).

The spatial domain for this analysis is the contiguous United States. InMAP employs a variable-resolution grid (i.e., for a given simulation, the cells making up the simulation spatial domain vary in size), with cells' edge lengths ranging from 1 to 288 km. We use "population-weighted average horizontal grid cell edge length" as a characteristic grid cell size for each simulation. Here we test five variable-resolution grids, with characteristic grid cell sizes ranging from 5.9 to 69 km (see Table S4). For all simulations, smaller grid cells are used in areas with larger gradients in population density and pollutant concentration (see Figure S1). In simulations with smaller grid cells on average, the size of each grid cell is determined according to successively lower thresholds in population density and pollutant concentration. Table S5 shows the fraction of the U.S. population contained in grid cells of each horizontal edge length for each simulation. The grid cell size containing the most population is 96 km for the coarsest grid and 4 km for the finest grid.

For each model run, InMAP estimates annual-average $PM_{2.5}$ concentrations in each grid cell. Population counts in each grid cell are determined in InMAP by area-weighted interpolation of population from the Block Group scale. We then calculate the population-weighted average $PM_{2.5}$ concentrations for each population subgroup by race-ethnicity and income (below, we use the term "exposure" to represent population-weighted average concentrations). The difference in average $PM_{2.5}$ exposure between these population subgroups provides a quantitative measure of environmental injustice. To check whether exposure differences by race-ethnicity are confounded by income differences, we calculate the income-adjusted disparity in exposure between white and minority populations

DOI: 10.1021/acs.estlett.8b00279
Environ. Sci. Technol. Lett. 2018, 5, 436−441

by performing a population-weighted average of within-income-category exposure differences:

$$\text{disparity} = \frac{1}{\sum_{k=1}^{16}(P_{M_k} + P_{W_k})} \sum_{k=1}^{16} \left[(P_{M_k} + P_{W_k}) \left(\left\{ \frac{1}{\sum_{i=1}^{n} P_{M_{k(i)}}} \sum_{i=1}^{n} [P_{M_{k(i)}} C_i] \right\} - \left\{ \frac{1}{\sum_{i=1}^{n} P_{W_{k(i)}}} \sum_{i=1}^{n} [P_{W_{k(i)}} C_i] \right\} \right) \right]$$

where C_i represents the $PM_{2.5}$ concentration in the ith grid cell, P_{M_k} and P_{W_k} represent the total minority and white populations, respectively, in the kth income category, and $P_{M_{k(i)}}$ and $P_{W_{k(i)}}$ represent the minority and white populations, respectively, in the kth income category and the ith grid cell. The number of grid cells, n, varies by simulation.

RESULTS AND DISCUSSION

Our five model runs simulate national annual-average $PM_{2.5}$ concentrations, for total $PM_{2.5}$ and for chemical subspecies, for the year 2014. Model runs employ between 1818 (coarse resolution) and 103098 (fine resolution) ground-level grid cells (see Table S4) with additional elevated grid cells.

Results suggest that model-estimated exposure disparities are sensitive to grid resolution for race-ethnicity but not income. Figure 1a shows that as the average grid cell size decreases, the estimated total $PM_{2.5}$ exposure increases for all four race-ethnicity groups, reflecting a correlation between population and $PM_{2.5}$ concentration (correlation coefficients are listed in Table S6). The effect of finer resolution on $PM_{2.5}$ exposure is nearly twice as large for minorities (difference between coarsest and finest grid resolution of 2.5 $\mu g\ m^{-3}$, a 36% increase) as for whites (1.3 $\mu g\ m^{-3}$, a 20% increase), which can be attributed in part to coarse grids smoothing out spatial clustering of minority populations (see Figure S2).

Across all grid resolutions, $PM_{2.5}$ exposure is lowest for whites. Upon comparison of the results of the coarsest- and finest-resolution grids, as shown in Figure 1b, the $PM_{2.5}$ exposure disparity between whites and minorities increases most for Asians (Asian vs white exposure difference of 0.1 $\mu g\ m^{-3}$ for the coarsest resolution vs 1.6 $\mu g\ m^{-3}$ for the finest resolution). As mentioned above, these trends can in part be attributed to the coarse grids smoothing out the spatial clustering of minority populations.

Figure 2 compares the impact of grid resolution on $PM_{2.5}$ exposure disparities by race-ethnicity and income. This figure shows that model-estimated disparities by income do not change dramatically for coarse- versus fine-resolution grids. In contrast, model-estimated disparities by race-ethnicity are substantially larger for fine-resolution than for coarse-resolution grids and are higher than disparities by income for all grids. Here, considering race-ethnicity only (Figure 2, blue line) versus income-adjusted differences by race-ethnicity (Figure 2, green line) yields nearly identical findings.

Figure 3 shows $PM_{2.5}$ exposure by income category (i.e., for the 16 household income categories in the U.S. Census) and how exposure estimates vary with grid resolution. At the coarsest-resolution grid (69 km), the minority versus white

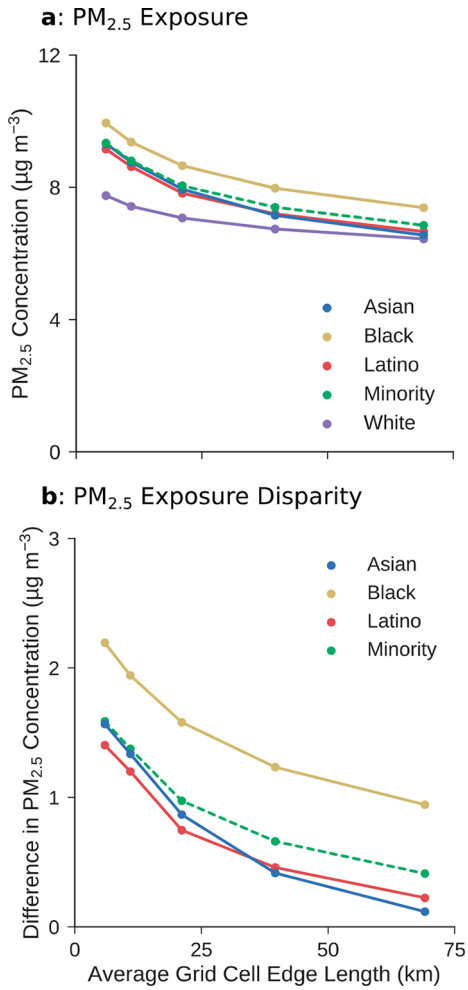

Figure 1. Differences by race-ethnicity and resolution in (a) average $PM_{2.5}$ exposure and (b) $PM_{2.5}$ exposure disparity (i.e., difference in average exposure for a population subgroup relative to whites). The dashed line represents the minority category, defined as the combination of Asian, black, Latino, and other groups not identifying as white.

exposure difference is <0.5 $\mu g\ m^{-3}$ in each income category (with the narrowest gap in the highest income category). The minority versus white exposure gap increases in each income category at the finest-resolution grid (5.9 km), with a weighted-average difference of 1.6 $\mu g\ m^{-3}$. Minority exposure is higher than white exposure within every income category, irrespective of grid resolution. These results demonstrate that while income is somewhat related to exposure differences (especially at the highest income levels), income cannot fully explain the racial-ethnic disparities in $PM_{2.5}$ pollution uncovered by a finer grid resolution (Tables S7 and S8 demonstrate that racial-ethnic characteristics are more correlated with $PM_{2.5}$ concentrations than are income characteristics).

Figure 4 shows the effect of finer grid resolution on the minority versus white exposure disparity, by $PM_{2.5}$ subspecies. We find that the minority versus white disparity in primary $PM_{2.5}$ concentrations is the most sensitive to grid resolution, with an increase of 0.7 $\mu g\ m^{-3}$ (183%) from the coarsest to finest resolution. While primary $PM_{2.5}$ accounts for 37% of estimated overall exposure (see Figure S3), it is responsible for 62% of the increase in minority versus white exposure disparity

DOI: 10.1021/acs.estlett.8b00279
Environ. Sci. Technol. Lett. 2018, 5, 436−441

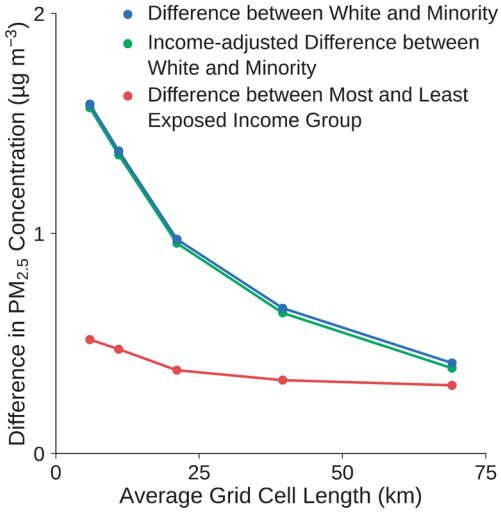

Figure 2. Total $PM_{2.5}$ exposure disparity, adjusting for income. These results indicate that for all five model resolutions studied, exposures are higher for minorities than for whites; differences by race-ethnicity are nearly identical for income-adjusted vs unadjusted results. For all model resolutions studied, the disparity by race-ethnicity exceeds the largest disparity between any two income categories. The most exposed income category is the category making less than $10000 for all grids. The least exposed income category is the category making $150000−199999 for the coarsest grid, the category making $125000−149999 for second and third coarsest grids, and the category making $75000−99999 for the two finest grids.

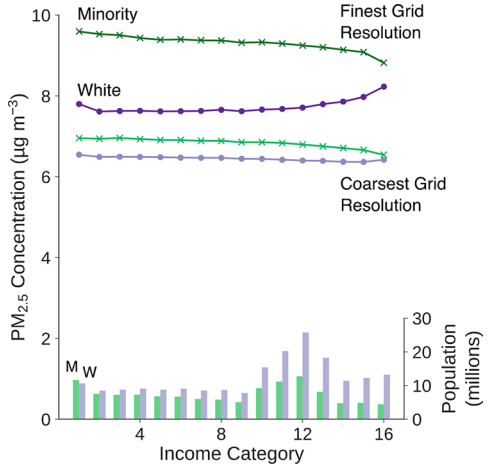

Figure 3. Minority (M) and white (W) $PM_{2.5}$ exposure as a function of income for the coarsest and finest grid resolutions (lines) and population in each income category (bars). Income categories range from less than $10000 to $200000 or more (see Table S3 for all income category descriptions).

in total $PM_{2.5}$ concentrations attributable to finer grid resolution. Disparities in concentrations of the other components of secondary $PM_{2.5}$ change by <0.2 $\mu g\ m^{-3}$. Prior work suggests that InMAP performance is better for primary $PM_{2.5}$, pSO_4, and secondary organic aerosol (SOA) than for particulate ammonium (pNH_4) and particulate nitrate (pNO_3).[27] Because formation of secondary $PM_{2.5}$ takes time (during which atmospheric mixing reduces pollutant spatial gradients), spatial concentration gradients tend to be greater for primary than for secondary $PM_{2.5}$, thereby increasing opportunities for exposures to be sensitive to model resolution.[25] This observation aligns with our results, and

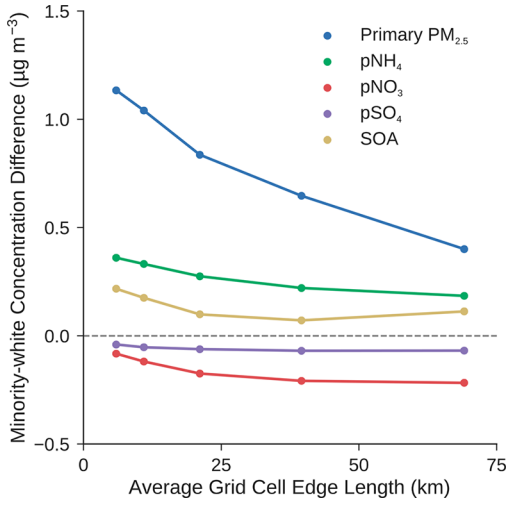

Figure 4. Minority vs white $PM_{2.5}$ exposure disparity by $PM_{2.5}$ species.

with the findings of Punger and West,[21] that estimates of exposure from $PM_{2.5}$ are more sensitive to spatial resolution for primary $PM_{2.5}$ than for secondary $PM_{2.5}$.

Our results provide evidence that coarse-resolution mechanistic models used to assess equity in air pollution exposure may underestimate disparities between white and minority populations. Furthermore, we find that the racial-ethnic disparities in exposure uncovered with fine spatial resolution can be detected for all income categories. As shown in Figure 1, we find a strong relationship among grid resolution, exposure, and especially exposure disparities. To the extent that baseline mortality rates and dose−response relationships vary among population subgroups, disparities in health impacts may be larger or smaller than exposure disparities. For example, in 2014, the CDC-estimated baseline age-adjusted mortality rates (deaths per year per 100000 people) for the racial-ethnic groups included in this study were 391 (Asian), 871 (black), 523 (Latino), and 743 (white).[32]

Important limitations of this study include the use of a reduced-complexity model, rather than a conventional chemical transport model (CTM). CTMs such as CMAQ[33] and CAMx[34] are typically more accurate than reduced-complexity models such as InMAP. In particular, InMAP models primary organic aerosol (POA) as nonvolatile primary $PM_{2.5}$, but recent research indicates complex POA dynamics involving evaporation, chemical reaction, and condensation; models that account for these dynamics often predict lower near-source concentrations of POA.[35] Investigating these dynamics as they relate to population exposure and exposure disparities is an area for future research. The accuracy of amounts and spatial locations of emissions provided in the NEI is an additional source of uncertainty in our results.

To evaluate the performance of the InMAP model, predicted total $PM_{2.5}$ concentrations were compared to observed annual-average concentrations at measurement locations[36] for each of the five spatial resolutions tested in this study and for an InMAP simulation with a 12 km uniform grid (see Table S9 and Figures S4−S9). The mean fractional bias is reduced from −39% at the coarsest-resolution grid (69 km) to −17% at the finest-resolution grid (5.9 km), while the mean fractional error decreases from 44 to 35%. The model R^2 increases from 0.16 to 0.26 as the average grid cell size decreases. These results suggest that performance does not diminish substantially with

DOI: 10.1021/acs.estlett.8b00279
Environ. Sci. Technol. Lett. 2018, 5, 436−441

finer-resolution grids. Performance evaluations were also conducted by $PM_{2.5}$ species for which measurement data matching InMAP model species were available. At the finest-resolution grid, the model R^2 is higher for pSO_4 (0.59) than for pNH_4 and pNO_3 (0.27 and 0.33, respectively). In contrast, the mean fractional bias and mean fractional error are close to ±100% for pSO_4, while they are less than ±60% for both pNH_4 and pNO_3 (see Figures S10−S27).

An advantage of InMAP is that, in contrast to CTM simulations using current computational technology, InMAP is able to predict $PM_{2.5}$ concentrations for the contiguous United States at a spatial resolution finer than the resolution that has been used in previous studies. Table S4 contains run times for each simulation. Previous CTM-based studies of the effect of varying spatial resolution on annual-average $PM_{2.5}$ exposure have employed a minimum grid cell size of 12 km for the contiguous United States or 4 km for local or regional scales,[21,24,37] whereas our finest-resolution InMAP simulation uses a minimum grid cell size of 1 km with a population-weighted average size of 5.9 km nationwide and 3.6 km in urbanized areas. For our finest-resolution grid, meteorological inputs are at a spatial resolution coarser than that of the model. Therefore, spatial smoothing of meteorological data (e.g., wind speed) may reduce model accuracy. Tessum et al.[27] compare predicted primary $PM_{2.5}$ concentrations at a 1 km spatial resolution in Los Angeles using InMAP (with 9 km WRF-Chem meteorology) and WRF-Chem (with 1 km meteorology), finding lower spatial gradients for concentrations modeled by InMAP in that case.

The primary goal of this analysis has been to investigate the relationship between grid resolution and exposure in a mechanistic air quality model. We use the year-2014 NEI emissions to represent typical emission locations and give a sense of the scale of exposure and exposure disparities; we do not intend this analysis to provide a definitive, present-day estimate of exposures and exposure disparities. Further research could usefully investigate the impact of grid resolution on (1) exposure for scenarios involving current or future emissions, (2) exposure in different regions or cities within the United States or other countries, or (3) exposure for other population subgroups.

■ ASSOCIATED CONTENT

Supporting Information

The Supporting Information is available free of charge on the ACS Publications website at DOI: 10.1021/acs.estlett.8b00279.

Supporting information information includes tables and figures detailing the literature review conducted for this study, information about population subgroup distributions, characteristics of the spatial grids used, correlations between population groups and pollutant concentration, and performance evaluations. (PDF)

■ AUTHOR INFORMATION

Corresponding Author

*E-mail: ctessum@uw.edu.

ORCID

David A. Paolella: 0000-0001-5737-2508

Joshua S. Apte: 0000-0002-2796-3478

Author Contributions

D.A.P., C.W.T., and J.D.M. conceived and designed the experiments. D.A.P., C.W.T., and J.D.M. analyzed the data. D.A.P., C.W.T., P.J.A., J.S.A., S.C., J.H., N.Z.M., and J.D.M. wrote the paper.

Notes

The authors declare no competing financial interest.

■ ACKNOWLEDGMENTS

The authors thank Elisabeth Gilmore, Neal Fann, and Bryan Hubbell for helpful discussions. This publication was developed under Assistance Agreement R835873 awarded by the U.S. Environmental Protection Agency. It has not been formally reviewed by EPA. The views expressed in this document are solely those of authors and do not necessarily reflect those of the Agency. EPA does not endorse any products or commercial services mentioned in this publication.

■ REFERENCES

(1) Landrigan, P. J.; Fuller, R.; Acosta, N. J. R.; Adeyi, O.; Arnold, R.; Basu, N.; Baldé, A. B.; Bertollini, R.; Bose-O'Reilly, S.; Boufford, J. I.; et al. The Lancet Commission on pollution and health. *Lancet* **2018**, *391*, 462.

(2) GBD Compare Data Visualization. Institute for Health Metrics and Evaluation (IHME), University of Washington, Seattle, 2017 (http://ghdx.healthdata.org/gbd-results-tool) (accessed October 31, 2017).

(3) Pope, C. A.; Dockery, D. W. Health Effects of Fine Particulate Air Pollution: Lines that Connect. *J. Air Waste Manage. Assoc.* **2006**, *56*, 709−742.

(4) Crouse, D. L.; Peters, P. A.; van Donkelaar, A.; Goldberg, M. S.; Villeneuve, P. J.; Brion, O.; Khan, S.; Atari, D. O.; Jerrett, M.; Pope, C. A.; et al. Risk of nonaccidental and cardiovascular mortality in relation to long-term exposure to low concentrations of fine particulate matter: A canadian national-level cohort study. *Environ. Health Perspect.* **2012**, *120*, 708−714.

(5) Brook, R. D.; Rajagopalan, S.; Pope, C. A.; Brook, J. R.; Bhatnagar, A.; Diez-Roux, A. V.; Holguin, F.; Hong, Y.; Luepker, R. V.; Mittleman, M. A.; et al. Particulate matter air pollution and cardiovascular disease: An update to the scientific statement from the American heart association. *Circulation* **2010**, *121*, 2331−2378.

(6) Cassee, F. R.; Mills, N. L.; Newby, D. E. Cardiovascular Effects of Inhaled Ultrafine and Nano-Sized Particles Cardiovascular Effects of Inhaled Ultrafine and Nano-Sized Particles. In *Cardiovascular Effects of Inhaled Ultrafine and Nano-Sized Particles*; Wiley: Hoboken, NJ, 2011; pp 24−83.

(7) Schwartz, J.; Coull, B.; Laden, F.; Ryan, L. The effect of dose and timing of dose on the association between airborne particles and survival. *Environ. Health Perspect.* **2008**, *116*, 64−69.

(8) Di, Q.; Wang, Y.; Zanobetti, A.; Wang, Y.; Koutrakis, P.; Choirat, C.; Dominici, F.; Schwartz, J. D. Air Pollution and Mortality in the Medicare Population. *N. Engl. J. Med.* **2017**, *376*, 2513−2522.

(9) Crouse, D. L.; Ross, N. A.; Goldberg, M. S. Double burden of deprivation and high concentrations of ambient air pollution at the neighbourhood scale in Montreal, Canada. *Soc. Sci. Med.* **2009**, *69*, 971−981.

(10) Bell, M. L.; Ebisu, K. Environmental inequality in exposures to airborne particulate matter components in the United States. *Environ. Health Perspect.* **2012**, *120*, 1699−1704.

(11) Miranda, M. L.; Edwards, S. E.; Keating, M. H.; Paul, C. J. Making the environmental justice grade: the relative burden of air pollution exposure in the United States. *Int. J. Environ. Res. Public Health* **2011**, *8*, 1755−1771.

(12) Grineski, S. E.; Collins, T. W.; Morales, D. X. Asian Americans and disproportionate exposure to carcinogenic hazardous air pollutants: A national study. *Soc. Sci. Med.* **2017**, *185*, 71−80.

DOI: 10.1021/acs.estlett.8b00279
Environ. Sci. Technol. Lett. 2018, 5, 436−441

(13) Clark, L. P.; Millet, D. B.; Marshall, J. D. National patterns in environmental injustice and inequality: Outdoor NO_2 air pollution in the United States. *PLoS One* **2014**, *9*, e94431.
(14) Jones, M. R.; Diez-Roux, A. V.; Hajat, A.; Kershaw, K. N.; O'Neill, M. S.; Guallar, E.; Post, W. S.; Kaufman, J. D.; Navas-Acien, A. Race/ethnicity, residential segregation, and exposure to ambient air pollution: The Multi-Ethnic Study of Atherosclerosis (MESA). *Am. J. Public Health* **2014**, *104*, 2130−2137.
(15) Marshall, J. D. Environmental inequality: Air pollution exposures in California's South Coast Air Basin. *Atmos. Environ.* **2008**, *42*, 5499−5503.
(16) Hajat, A.; Hsia, C.; O'Neill, M. S. Socioeconomic Disparities and Air Pollution Exposure: a Global Review. *Curr. Environ. Heal. reports* **2015**, *2*, 440−450.
(17) Rosofsky, A.; Levy, J. I.; Zanobetti, A.; Janulewicz, P.; Fabian, M. P. Temporal trends in air pollution exposure inequality in Massachusetts. *Environ. Res.* **2018**, *161*, 76−86.
(18) Fann, N.; Roman, H. A.; Fulcher, C. M.; Gentile, M. A.; Hubbell, B. J.; Wesson, K.; Levy, J. I. Maximizing Health Benefits and Minimizing Inequality: Incorporating Local-Scale Data in the Design and Evaluation of Air Quality Policies. *Risk Anal.* **2011**, *31*, 908−922.
(19) Pinault, L.; Crouse, D.; Jerrett, M.; Brauer, M.; Tjepkema, M. Spatial associations between socioeconomic groups and NO_2 air pollution exposure within large Canadian cities. *Environ. Res.* **2016**, *147*, 373−382.
(20) Executive Order 12898 of February 11, 1994: Federal Actions To Address Environmental Justice in Minority Populations and Low-Income Populations. *Federal Register*; Office of the Federal Register: Washington, DC, 1994 (http://www.archives.gov/federal-register/executive-orders/pdf/12898.pdf) (accessed October 22, 2017).
(21) Punger, E. M.; West, J. J. The effect of grid resolution on estimates of the burden of ozone and fine particulate matter on premature mortality in the USA. *Air Qual., Atmos. Health* **2013**, *6*, 563−573.
(22) Li, Y.; Henze, D. K.; Jack, D.; Kinney, P. L. The influence of air quality model resolution on health impact assessment for fine particulate matter and its components. *Air Qual., Atmos. Health* **2016**, *9*, 51−68.
(23) Kodros, J. K.; Wiedinmyer, C.; Ford, B.; Cucinotta, R.; Gan, R.; Magzamen, S.; Pierce, J. R. Global burden of mortalities due to chronic exposure to ambient PM 2.5 from open combustion of domestic waste. *Environ. Res. Lett.* **2016**, *11*, 124022.
(24) Thompson, T. M.; Saari, R. K.; Selin, N. E. Air quality resolution for health impact assessment: Influence of regional characteristics. *Atmos. Chem. Phys.* **2014**, *14*, 969−978.
(25) Guidance on the Use of Models and Other Analyses for Demonstrating Attainment of Air Quality Goals for Guidance on the Use of Models and Other Air Quality Goals for Ozone, PM2.5, and Regional Haze. Technical Report EPA-454/B-07-002; U.S. Environmental Protection Agency: Research Triangle Park, NC, 2007 (https://www3.epa.gov/scram001/guidance/guide/final-03-pm-rh-guidance.pdf) (accessed June 23, 2017).
(26) Saari, R. K.; Thompson, T. M.; Selin, N. E. Human Health and Economic Impacts of Ozone Reductions by Income Group. *Environ. Sci. Technol.* **2017**, *51*, 1953−1961.
(27) Tessum, C. W.; Hill, J. D.; Marshall, J. D. InMAP: A model for air pollution interventions. *PLoS One* **2017**, *12*, e0176131.
(28) *National Emissions Inventory (NEI) version 1, 2014*; Office of Air Quality Planning and Standards, Emissions Inventory Group; Emissions, Monitoring and Analysis Division, U.S. Environmental Protection Agency: Washington, DC, 2016.
(29) Assigning sources to grid cells. *SMOKE version 4.5 User Manual*; section 2.12.2, 2017 (https://www.cmascenter.org/smoke/documentation/4.5/html/ch02s12s02.html).
(30) *Air Emissions Processor (AEP) Computer Program*; https://github.com/ctessum/aep (accessed April 19, 2018).
(31) Manson, S.; Schroeder, J.; Van Riper, D.; Ruggles, S. *IPUMS National Historical Geographic Information System*, version 12.0 (Database); University of Minnesota: Minneapolis, 2017 (https://www.nhgis.org) (accessed July 31, 2017).
(32) Underlying Cause of Death 1999−2015. National Center for Health Statistics, Centers for Disease Control and Prevention: Atlanta, 2016 (http://wonder.cdc.gov/ucd-icd10.html) (accessed December 19, 2017).
(33) Byun, D. W.; Ching, J. K. S. Science Algorithms of the EPA Models-3 Community Multiscale Air Quality (CMAQ) Modeling System. Technical Report EPA/600/R-99/030; U.S. Environmental Protection Agency: Washington, DC, 1999 (www.epa.gov/cmaq) (accessed August 28, 2017).
(34) *ENVIRON. User's Guide: Comprehensive Air-Quality Model with Extensions*; ENVIRON International Corp.: Novato, CA, 2011 (http://www.camx.com/files/camxusersguide_v6-40.pdf) (accessed August 28, 2017).
(35) Robinson, A. L.; Donahue, N. M.; Shrivastava, M. K.; Weitkamp, E. A.; Sage, A. M.; Grieshop, A. P.; Lane, T. E.; Pierce, J. R.; Pandis, S. N. Rethinking organic aerosols: Semivolatile emissions and photochemical aging. *Science* **2007**, *315*, 1259−1262.
(36) AirData. U.S. Environmental Protection Agency: Washington, DC, 2014 (https://aqs.epa.gov/aqsweb/airdata/download_files.html) (accessed March 5, 2018).
(37) Arunachalam, S.; Wang, B.; Davis, N.; Baek, B. H.; Levy, J. I. Effect of chemistry-transport model scale and resolution on population exposure to PM2.5 from aircraft emissions during landing and takeoff. *Atmos. Environ.* **2011**, *45*, 3294−3300.

DOI: 10.1021/acs.estlett.8b00279
Environ. Sci. Technol. Lett. 2018, 5, 436−441